

Fractional frequency parametric resonances in a Paul trap

M. A. N. Razvi^{a,b}, X. Z. Chu^{a,c}, R. Alheit^a, R. Blümel^d and G. Werth^a

^a*Institut für Physik, Johannes-Gutenberg-Universität, D55099 Mainz, Germany*

^b*Spectroscopy Division, Bhabha Atomic Research Centre, Trombay, Mumbai 400 085, India*

^c*Department of Electrical and Computer Engineering,*

University of Illinois, 1308 West Main Street, Urbana, IL 61801-2307

^d*Fakultät für Physik, Albert-Ludwigs-Universität, Hermann-Herder-Str. 3, D-79104 Freiburg, Germany*

Abstract. Excitation of the motional frequencies of clouds of H_2^+ and N_2^+ ions, confined in a Paul trap, by an additionally applied radiofrequency quadrupole field leads to the observation of parametric resonances that are predicted to occur at frequencies $2\omega_z/n$, $n = 1, 2, 3, \dots$, where ω_z is the axial secular frequency. In the case of clouds of N_2^+ ions resonances up to $n = 10$ are detected. They can be explained by parametric instabilities of the center-of-mass motion in the axial direction. The fractional resonances are observable only if the excitation field surpasses a critical strength. We find an odd-even staggering of the thresholds.

I. INTRODUCTION

In addition to its use as a tool in spectroscopy, the Paul trap is an ideal device for the investigation of nonlinear dynamics and complex systems. Many effects initially observed experimentally in Paul traps were eventually explained within the framework of nonlinear dynamics and chaos. Examples are the phenomenon of rf heating [1] and crystallization and melting of Coulomb crystals [2–6]. Another example of a complex system where nonlinear dynamics plays a role are large clouds of H_2^+ or N_2^+ ions stored in a Paul trap under the influence of an additionally applied excitation quadrupole field whose frequency ω is scanned [7,8]. Interesting resonance doublets appear in the vicinity of the discrete excitation frequencies $\omega_n = 2\omega_z/n$, $n = 1, 2, 3, \dots$. Our experiments show that one of the resonances in the doublet appears only if the excitation voltage surpasses a threshold value that depends on n . The dependence of the threshold voltage on n is rather peculiar and depends on whether n is even or odd. We call this effect “odd-even staggering” [8]. While we succeeded in explaining most of the features of the resonance doublet at least qualitatively, including the very existence of a threshold voltage, we have not yet succeeded in explaining the odd-even staggering effect.

II. EXPERIMENTAL SETUP AND PROCEDURES

A schematic sketch of our set-up is shown in Fig. 1. Most of the components of our experiment are described in detail in [9,10]. In our current experiments we use a Paul trap with an inner radius of the ring electrode of $r_0 = 2$ cm and end-cap distance of $2z_0 = \sqrt{2}r_0$. The trap is operated at a frequency of $\Omega/2\pi = 3$ MHz.

In order to study the nonlinear response of large ion clouds stored in the Paul trap to an additionally applied ac excitation voltage we measure the survival rate of the ions in the presence of the excitation field for well defined excitation frequency, amplitude and interaction time. We refer to this type of experiments as excitation experiments. A typical excitation experiment consists of three stages.

(i) Creation stage

In this stage, of temporal duration T_c , the ions are created inside the trap by electron bombardment of the rest gas which is held at 10^{-9} mbar. We refer to T_c as the creation time. It is typically of the order of 1 s.

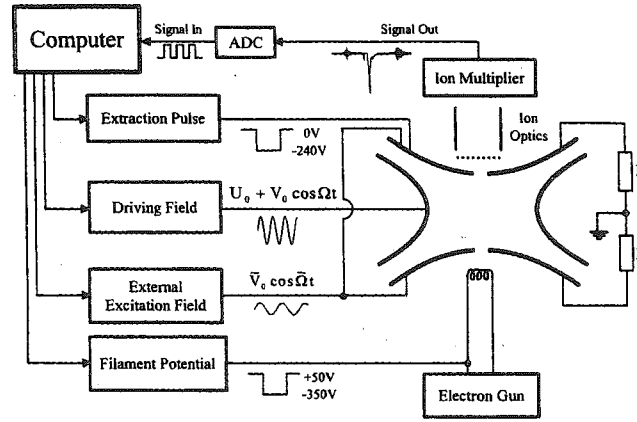


FIGURE 1. Sketch of the experimental set-up.

(ii) *Interaction stage*

After creating the ions, they are exposed to a superposition of the trap fields and the excitation field during a time T_i , referred to as the interaction time. The interaction time T_i can be changed experimentally from a few ms to arbitrarily long times. In practice, however, an upper limit of T_i is given by the ion storage time which is typically of the order of 8–10 s under our experimental conditions. During the interaction stage both end caps of the trap are electrically connected. This observation is important, since it rules out dipole excitation of the ion clouds.

(iii) *Detection stage*

Following the interaction stage, we extract the ions with the help of a field pulse through the upper end cap of the trap. The extraction pulse is phase correlated with the trap's ac driving field. The ions arrive at the first dynode of a multiplier tube and create an electron pulse whose total charge is proportional to the ion number. The pulse is amplified and digitized and fed to a PC for further data handling. Different mass ions arrive at the detector at different times. A particular species of ions (e.g. H_2^+ or N_2^+ ions) is selected by setting an amplifier gate at proper timing. The total detection efficiency including ion loss in the time-of-flight region and quantum efficiency of the multiplier is estimated to be 10%.

A motional resonance is detected by a decrease of the ion number arriving at the detector. We should emphasize that for every data point in our experimental observations, the ions are lost from the trap and new ions have to be created for the next point. Thus the ions under investigation do not have a “memory” concerning previous excitations. This is of importance for the shape of the observed resonances.

III. THEORETICAL PRELUDE: WHAT TO EXPECT?

For a first qualitative analysis of a system as complex as an externally excited ion cloud in a Paul trap it is best to resort to the simplest possible model in the hope to capture qualitatively the most prominent effects. Following this recipe we focus only on the center-of-mass coordinates (X, Y, Z) of the ion cloud. Moreover, since in our experiments we investigated mainly axial excitations of the stored ions, we retain only the Z coordinate. In the pseudopotential approximation [1] the equation of motion of the Z coordinate of the cloud perturbed by the additional excitation voltage reads

$$\ddot{Z} + \omega_z^2 Z = F \cos(\omega t) Z, \quad (1)$$

where ω_z is the axial pseudopotential frequency and F is the strength of the additionally applied excitation field. The substitution $\tau = \omega t/2$ turns (1) into the Mathieu equation

$$\ddot{Z} + [a - 2q \cos(2t)] Z = 0, \quad (2)$$

where $a = (2\omega_z/\omega)^2$ and $q = 2F/\omega^2$ are the control parameters of the Mathieu equation. Note that (1) is not the equation of motion of an ordinary driven harmonic oscillator, since Z occurs on the right hand side of the equation. Thus, independently of F , $Z = 0$ is always a solution of (1) and (2). Appreciable amplitudes Z accompanied by

appreciable particle loss can be obtained only for a and q combinations which turn the fixed point $Z = 0$ of (2) unstable. It is known from the theory of the Mathieu equation [11] that for small q the Mathieu equation (2) is unstable for $a = n^2$. It follows that (1) is unstable for $\omega_n = 2\omega_z/n$, $n = 1, 2, 3, \dots$. These instabilities are also called parametric instabilities. Based on this simple theory we obtain a first prediction: Large particle loss at frequencies in the vicinity of the parametric instabilities at ω_n .

So far the theory was Hamiltonian, i.e. no damping was present. In an experiment, however, damping cannot be avoided. Appropriate scaling of the time variable and the addition of a damping term turns (1) into

$$\ddot{Z} + \gamma\dot{Z} + Z = f \cos(\nu\tau)Z. \quad (3)$$

Here γ is the damping constant, f is the scaled excitation strength, ν is the scaled excitation frequency, τ is the scaled time and the dot refers to differentiation with respect to τ . Addition of the damping term changes the qualitative features of the theory. While in the theory without damping 100% particle loss occurs in the parametric instability regions, in the presence of damping the fixed point $Z = 0$ of (3) is stable for small enough, but nonzero f . Thus, in order to induce particle loss at $\omega \approx \omega_n$, f has to exceed a *threshold* f_n . According to a formula stated without derivation in Landau and Lifshitz [12] the critical excitation strength f_n is given by

$$f_n = \alpha_n(\gamma)\gamma^{1/n}. \quad (4)$$

We checked in various representative cases that $\alpha_n(\gamma)$ depends only weakly on n and γ .

A last comment concerns the efficiency of the expected particle loss as a function of the excitation frequency ω . Apparently the particle loss from the cloud is the more efficient the larger the amplitude Z will turn out in the parametric instability regions. In the case of an ideal Paul trap the trapping field is an ideal quadrupole, and in the parametric instability region Z grows exponentially in time without bounds. This holds even in the presence of damping. But in a real Paul trap there are always field imperfections present which add nonlinearities to the trapping field. These nonlinearities limit the maximally achievable amplitude Z at given excitation strength F . Again we refer to Landau and Lifshitz who predict that the form of Z in the regions of parametric instability has a peculiar saw-tooth shape [12], rising sharply, but continuously from $Z = 0$ at the beginning of the instability and falling to zero sharply and discontinuously at the end of the instability. This behavior translates immediately into a prediction for the shape of the particle-loss curve as a function of ω : we should see a saw-tooth shaped particle-loss curve.

In summary, based on the simple theory of parametric instability, we should observe the following three effects: (i) Large particle loss at ω_n , (ii) a saw-tooth shaped particle loss curve and (iii) excitation thresholds that follow the law: $f_n \approx \alpha\gamma^{1/n}$.

IV. EXPERIMENTAL RESULTS

We now compare the theoretical predictions with the results of our excitation experiments described in Section II. For the case of a cloud of H_2^+ ions, Fig. 2 shows the number of surviving ions as a function of the excitation frequency in the vicinity of the $n = 1$ parametric instability. Surprisingly, instead of the single expected instability resonance we obtain a doublet of two resonances, a broad one and a narrow one. A detailed analysis showed that it is the narrow resonance of the doublet that is described by the model of the center-of-mass motion [7]. Thus we called this resonance the “collective resonance” [7]. The broad resonance is explained by the same phenomenon, parametric instability, but now on the level of every single particle in the cloud. In addition to the trap fields, the particles in the cloud also see the space charge of the cloud and the position of the parametric resonance is thus shifted depending on the positions of the individual ions in the cloud. This gives rise to the incoherent part of the doublet and results in a broad resonance feature. Nevertheless, apart from the doublet nature of the parametric resonance, the experiment confirms the predicted instability at $\omega \approx \omega_1$. Figure 2 also confirms our second prediction, namely the saw-tooth shape of the resonance. This shape is clearly seen in the collective part of the resonance doublet in Fig. 2.

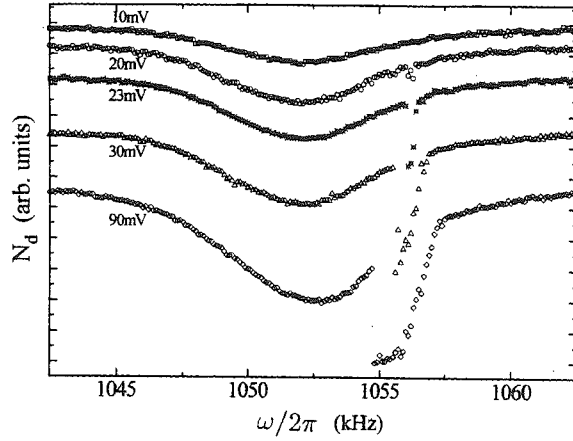


FIGURE 2. Number of detected H_2^+ ions in the vicinity of the $n = 1$ parametric resonance as a function of the excitation frequency for five different excitation voltages. The initial number of ions for the five different curves are the same. We shifted the curves vertically for clarity of presentation.

Recently we also observed the parametric instabilities for $n = 1, 2, \dots, 10$ in the case of large clouds of N_2^+ ions. A scan showing these resonances is presented in Fig. 3.

Another prediction of the theory is the existence of excitation thresholds due to the presence of damping. Our experiments confirm the existence of thresholds. This is demonstrated, e.g., in Fig. 2 which shows that in this case efficient excitation starts only for excitation voltages around 20 mV with no excitation at 10 mV and lower. Our experiments with clouds of N_2^+ ions confirm the existence of thresholds also for the higher order parametric resonances ($n = 2, \dots, 10$).

We now turn to a check of the threshold law $f_n = \alpha\gamma^{1/n}$. According to this law, plotting the logarithms of the measured critical excitation voltages versus $1/n$ should result in a collection of data points that essentially fall onto a single straight line with a shift that is associated with α and a slope given by $\log(\gamma)$. Figure 4 shows the experimental result. Instead of the expected single line, the data points fall onto two different straight lines depending on whether n is even or odd. This effect was called “odd-even staggering” in [8]. The reason for this effect is currently not known. On the basis of the threshold law $f_n = \alpha\gamma^{1/n}$ the staggering can be interpreted as a manifestation of two vastly different damping constants, $\gamma \approx 2 \times 10^{-3}$ for odd and $\gamma \approx 10^{-6}$ for even n , respectively. The constant of proportionality α , however, appears to be the same for both curves, since they intersect at $1/n \approx 0$.

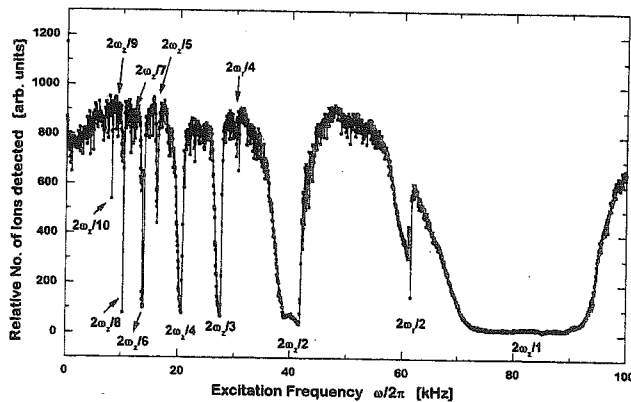


FIGURE 3. Experimental signatures of the first ten fractional parametric resonances for large clouds of N_2^+ ions.

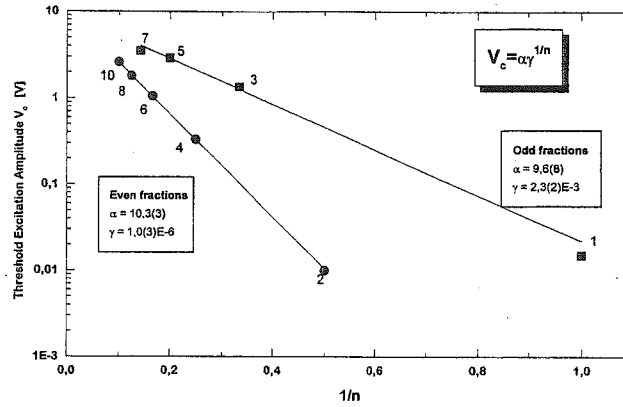


FIGURE 4. The logarithms of the measured critical (peak-to-peak) voltages V_c versus $1/n$ for fractional resonances of order $n = 1, 2, \dots, 10$ for N_2^+ ions. The solid line shows a least squares fit of the experimental data points by the function $V_c = \alpha\gamma^{1/n}$. The data point for $n = 9$ is missing due to experimental problems.

ACKNOWLEDGMENTS

The experiment was supported by the Deutsche Forschungsgemeinschaft. M. A. N. R. is grateful for financial support from the DLR International Buro's Indo-German bilateral scientific exchange program. X. Z. C. acknowledges a grant from the Deutscher Akademischer Austauschdienst. R. B. gratefully acknowledges financial support by the Deutsche Forschungsgemeinschaft (SFB 276).

REFERENCES

1. Dehmelt, H., *Adv. At. Mol. Phys.* **3**, 53-72 (1967).
2. Diedrich, F., Peik, E., Chen, J. M., Quint, W., and Walther, H., *Phys. Rev. Lett.* **59**, 2931-2934 (1987).
3. Wineland, D. J., Bergquist, J. C., Itano, W. M., Bollinger, J. J., and Manney, C. H., *Phys. Rev. Lett.* **59**, 2935-2938 (1987).
4. Hoffnagle, J., DeVoe, R. G., Reyna, L., and Brewer, R. G., *Phys. Rev. Lett.* **61**, 255-258 (1988).
5. Blümel, R., Chen, J. M., Peik, E., Quint, W., Schleich, W., Shen, Y. R., and Walther, H., *Nature (London)* **334**, 309-313 (1988).
6. Blümel, R., Kappler, C., Quint, W., and Walther, H., *Phys. Rev. A* **40**, 808-823 (1989).
7. Alheit, R., Chu, X. Z., Hofer, M., Holzki, M., Werth, G., and Blümel, R., *Phys. Rev. A* **56**, 4023-4031 (1997).
8. Razvi, M. A. N., Chu, X. Z., Alheit, R., Werth, G., and Blümel, R., *Phys. Rev. A* **58**, R34-R37 (1998).
9. Alheit, R., Hennig, C., Morgenstern, R., Vedel, F., and Werth, G., *Appl. Phys. B* **61**, 277-283 (1995).
10. Alheit, R., Gudjons, Th., Kleinedam, S., and Werth, G., *Rapid Comm. Mass Spectrom.* **10**, 583-590 (1996).
11. Abramowitz, M., and Stegun, I. A., *Handbook of Mathematical Functions*, Washington DC: National Bureau of Standards, 1964.
12. Landau, L. D., and Lifshitz, E. M., *Mechanics*, Oxford: Pergamon Press, 1960.